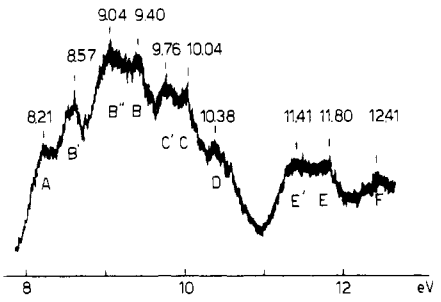

Figure 12. He I PE spectrum of $Os_2(CO)_6(C_4H_4)$.

competitive with the M → π_3*(C_4H_4) and M → π*(semibridging CO) back-donations. An even stronger metal–metal interaction is expected and actually computed for **III** (Table I). On this basis, one could tentatively explain the sawhorse geometry of **III**, because no semibridging carbonyl is now necessary to balance metal charges. The very strong metal–metal bond is consistent with the Os–Os′ bond length (2.75 Å),[5j] which is shorter than those observed in many cluster compounds,[28] including $Os_3(CO)_{12}$ itself (2.88 Å).[28d,e] It is of relevance to point out that almost all a′ type MOs participate in the metal–metal bond with a large contribution from the HOMO (see relative CP in Figure 11).

The experimental PE pattern of **III** below 12.5 eV (see Figure 12) is much more structured than those of **I** and **II**. The assignments are quite straightforward by reference to the discussion of **I** and **II** and to the TSIEs of Figure 2. In Figure 12 one can single out at least 10 well-resolved bands. Band A is once again assigned to the ionization from the HOMO 29a′, while band B′ is related to the ionization from the 19a″ MO. The existence of the resolved band B′ in **III** supports the theoretically expected antibonding interaction between the nd AO and ligand-based orbitals becoming stronger along the series Fe → Ru → Os. Bands B and C are both split into two components (B″, B and C′, C, respectively) with relative intensity 2:1:1:1. Believing in the TSIE ordering obtained by the present nonrelativistic calculations, one could tentatively assign band B″ to the ionization from the 28a′ and 18a″ MOs, while the three subsequent bands could be associated with the ionizations from the 27a′, 26a′, and 17a″ MOs, respectively. Band D should be assigned to the ionization from the 25a′ MO, and bands E′, E, and F are associated with single ionization events (24a′, 16a″, and 23a′ MOs, respectively).

Concluding Remarks

The present study has demonstrated that in polynuclear organometallic molecules the strength of the metal–metal bond can influence the nature of the metal–ligand interactions. Actually, in the present series of isoelectronic molecules, where only metals of the same group have been changed, significantly different bonding schemes have been found. Such differences have been traced back ultimately to differences in metal electronegativity and nd AO size. The role played by electronegativity is confirmed by structural data of a related heterobinuclear (Fe–Ru) cluster,[5h,29] where the metalla position is always occupied by the Ru atom, being less disposable than Fe in the formation of a dative metal–metal bond. Similar considerations have been previously invoked to explain the structure of $M_2M'(CO)_9(RC_2R)$ (M = Fe, M′ = Ru, R = C_6H_5; M = Fe, M′ = Ru, R = C_2H_5),[29] $H_2Os_3(CO)_9(RC_2R)$ (R = CH_3),[30] and $Fe_3(CO)_9(RC_2R)$ (R = CH_3)[31] complexes.

Acknowledgment. Financial support for this study from the Ministero della Pubblica Istruzione (Rome) is gratefully acknowledged. We thank F. De Zuane for technical assistance.

Registry No. $Fe_2(CO)_6(C_4H_4)$, 108034-90-8; $Ru_2(CO)_6(C_4H_4)$, 108034-91-9; $Os_2(CO)_6(C_4H_4)$, 108034-92-0.

(28) (a) Ferraris, G.; Gervasio, G. *J. Chem. Soc., Dalton Trans.* **1972**, 1057. (b) Bradford, C. W.; Nyholm, R. S.; Gainsford, G. J.; Guss, J. M.; Ireland, P. R.; Mason, R. *J. Chem. Soc., Chem. Commun.* **1972**, 87. (c) Deeming, A. J.; Underhill, M. *J. Chem. Soc., Chem. Commun.* **1973**, 277. (d) Corey, E. R.; Dahl, L. F. *Inorg. Chem.* **1962**, *1*, 521. (e) Churchill, M. R.; DeBoer, B. G. *Inorg. Chem.* **1977**, *16*, 878.

(29) Busetti, V.; Granozzi, G.; Aime, S.; Gobetto, R.; Osella, D. *Organometallics* **1984**, *3*, 1510.

(30) Bertoncello, R.; Granozzi, G.; Busetti, V.; Aime, S.; Gobetto, R.; Osella, D. *Inorg. Chem.* **1986**, *25*, 4004.

(31) Granozzi, G.; Tondello, E.; Casarin, M.; Aime, S.; Osella, D. *Organometallics* **1983**, *2*, 430.

Contribution from the Laboratoires de Chimie (UA CNRS 1194) et Service de Physique, Dêpartement de Recherche Fondamentale, CENG, 85X F 38041 Grenoble Cédex, France

Structural and Magnetic Properties of a Novel Pentacopper(II) Cluster Involving a Trinucleating Catechol Ligand

Eric Gojon,[1a] Jacques Gaillard,[1b] Jean-Marc Latour,*[1a] and Jean Laugier[1b]

Received October 15, 1986

The structure of $Cu_5(OH)_2(L)_2(NO_3)_4 \cdot 2.5H_2O$, where H_2L is the new ligand 3,6-bis((4-methylpiperazino)methyl)pyrocatechol, has been determined by X-ray diffraction techniques to a final discrepancy index of $R = 0.049$. The complex crystallizes in the space group $P2_1/n$ with four molecules per unit cell having the dimensions $a = 15.559$ (3) Å, $b = 13.417$ (3) Å, $c = 24.638$ (8) Å, and $\beta = 99.03$ (1) °. The five copper atoms are arranged as a rectangular based pyramid. The copper atoms at the short edges of the rectangle are bridged by a hydroxide while those at the long edges are bridged by the catecholate ligand. The apical copper is bridged to each of the other copper atoms by a catecholate oxygen. Magnetic susceptibility data over the range 5–300 K and EPR experiments near helium temperature have been used to investigate the magnetic interactions within the pentanuclear cluster. The hydroxide-bridged coppers experience exchange interactions of ca. −80 and −145 cm^{-1} while the apical copper is more weakly coupled to the four others. These results are discussed with the help of the magnetic orbital concept.

Introduction

Catechols are ubiquitous in biology where they can act as electron donors,[2] complexing agents in carrier proteins,[3] and substrates, intermediates, or products of oxidative reactions.[4] In most of these processes, the catechols are found to interact with transition-metal ions, iron and copper mainly. This has led, in the recent past, to a surge of interest in transition-metal catecholates.[5] Solution studies have demonstrated the high affinity of catecholates for the cupric ion, especially when nitrogen ligands are associated with catechols in the copper coordination sphere.[6] Most of the early work was aimed at studying the copper-catalyzed

(1) (a) Laboratoires de Chimie. (b) Service de Physique.

(2) Reinhammar, B. In *Copper Proteins and Copper Enzymes*; Lontie, R., Ed., CRC Press: Boca Raton, FL, 1984; Vol. III, Chapter 1, pp 1–35.

(3) Raymond, K. N.; Carrano, C. J. *Acc. Chem. Res.* **1979**, *12*, 183–190.

(4) (a) Lerch, K. *Met. Ions Biol. Syst.* **1981**, *13*, 143–186. (b) Que, L. *Struct. Bonding (Berlin)* **1980**, *40*, 39–72.

(5) Pierpont, C. G.; Buchanan, R. M. *Coord. Chem. Rev.* **1981**, *38*, 45–87.

(6) Sigel, H. *Inorg. Chem.* **1980**, *19*, 1411–1413.

0020-1669/87/1326-2046$01.50/0 © 1987 American Chemical Society

oxidative transformation of catechols either from synthetic or biological points of view. Along these lines, a few copper complexes have been isolated in the past decade.[7-14] However, structural characterizations of this kind of compound have long been overdue and are just beginning to appear.[12-14] Thompson[12a] and Buchanan and Pierpont[14] have solved the structures of copper complexes of di-*tert*-butylsemiquinone and di-*tert*-butylcatechol, respectively, with diamines as coligands. In these products, the catechol and semiquinone chelate the metal ion. On the other hand, Karlin has prepared the tetrachlorocatecholate adduct of a (μ-phenoxo)dicopper complex. In this species, the catechol is no longer chelating but bridges the two copper atoms.[13]

In the course of a study of multinuclear complexes of redox-active ligands, we investigated the possibility of synthesizing copper catecholates in which the catechol does not chelate the metal, which leaves an equatorial coordination site open to exogeneous ligand binding. In order to divert the catechol from its "normal" chelating bonding mode, we used complexing side arms bearing nitrogen donors. Very recently we described the structural and magnetic properties of a novel tetranuclear copper(II) bis(catecholate) complex in which each catechol ligand chelates one copper atom and bridges two other copper atoms.[15] In this contribution we present the synthesis, the structure determination and the magnetic susceptibility and EPR spectroscopy studies of a novel pentacopper(II) bis(catecholate) complex involving a trinucleating catecholate ligand.

Experimental Section

General Methods. All chemicals and solvents were reagent grade and used as received. EPR spectra were recorded on a Varian E 109 spectrometer operating at X-band. Variable-temperature measurements were conducted by using an Oxford Instruments cryogenic temperature control apparatus (ESR 900). NMR data were obtained with a Bruker AM200 spectrometer. Magnetic susceptibility measurements were done with a variable-temperature superconducting SHE 900 magnetometer operating at 5 kG in the range 5–300 K. Diamagnetic corrections were evaluated by using Pascal's constants. The data were least-squares fitted to the equations indicated in the text. The quantity minimized in the fitting process was $\sum[\chi_{obsd}T - \chi_{calcd}T]^2$. The quality of the fit was estimated through the statistical indicator

$$R = \frac{\sum[\chi_{obsd}T - \chi_{calcd}T]^2}{N\sum[\chi_{obsd}T]^2}$$

where N is the number of measurements. R amounted to 3.0×10^{-6} for the calculation with eq 1 (see text) and 2.6×10^{-6} when Hamiltonian 2 is used.

Preparation of H_2L. In a three-neck flask, 12 g of paraformaldehyde and 40 g (0.40 mol) of *N*-methylpiperazine are dissolved in 120 cm^3 of 2-(2-ethoxyethoxy)ethanol and 120 cm^3 of benzene. The reaction mixture is brought to reflux and 35 cm^3 of solution is distilled. A 22-g (0.20-mol) sample of catechol is then added in 50 cm^3 of methanol. Then 150 cm^3 of the solution is distilled and the mixture is refluxed for 15 h to give a dark brown solution. This solution is extracted with 14 × 200 cm^3 of heptane. After the solvent has been stripped off, 118 g of a yellow-orange oil is obtained. The 2-(2-ethoxyethoxy)ethanol is distilled under vacuum at ca. 2 mmHg. The brown residue is solubilized in diethyl ether and left at −20 °C for several hours. Upon filtration 20.4 g (yield 30.5%) of H_2L is obtained as a white powder. Anal. Calcd for $C_{15}H_{30}N_4O_2$: C, 64.64; H, 9.04; N, 16.75; O, 9.57. Found: C, 64.7; H, 9.1; N, 16.7; O, 9.6. Mass spectrometry: molecular ion ($M^{\bullet+}$) 334, [M − (piperazineH)]$^{\bullet+}$ 234. ^{1}H NMR: δ 9.6 (s broad, 2 H, OH), 6.4 (s, 2 H, aromatic), 3.7 (s, 4 H, benzylic), 2.6 (s broad, 16 H, ethylic), 2.3 (s, 6 H, methylic) ^{13}C NMR; δ 145.7 (C1), 121.1 (C2), 118.6 (C3), 61.8 (C4), 55.0 (C6), 52.5 (C5), 45.9 (C7).

Preparation of $Cu_5(OH)_2(L)_2(NO_3)_4 \cdot 2.5H_2O$. In a three-neck flask, 1.5 g (4.48 mmol) of ligand is dissolved in 100 cm^3 of methanol under argon. Then 1 g (9.88 mmol) of triethylamine in 50 cm^3 of methanol is added, and the mixture is refluxed for 30 mn. A solution of 2.18 g (9.02 mmol) of copper nitrate in 100 cm^3 of methanol is then added. The resulting dark green mixture is refluxed for 2.5 h. After being cooled down to room temperature, the reaction mixture is filtered to eliminate a small amount of a brownish precipitate and the resulting clear solution is concentrated slightly and left at ambient temperature. After several days green crystals have formed and are collected by filtration. Anal. Calcd for $C_{36}H_{63}N_{12}O_{20.5}Cu_5$: C, 33.02; H, 4.85; N, 12.83; O, 25.04; Cu, 24.26. Found: C, 32.7; H, 5.1; N, 12.6; O, 25.0; Cu, 24.6.

X-ray Data Collection and Structure Solution and Refinement for $Cu_5(OH)_2(L)_2(NO_3)_4 \cdot 2.5H_2O$. A prismatic crystal of dimensions 0.15 × 0.15 × 0.30 mm was mounted on a Nonius CAD-4 diffractometer operating with the Mo Kα radiation and a graphite monochromator. Table I lists the experimental conditions and crystallographic informations. The cell parameters were refined from the angular positions of 25 reflections. The data were corrected for Lorentz and polarization effects but uncorrected for absorption. The structure was solved by direct methods and successive Fourier-differences with the program SHELX76.[16] The cluster, two water molecules, and three out of four nitrates were located easily. The position of the last nitrate was deduced from residual density peaks in the Fourier-difference maps, which occured in two separate regions of the cell. One of these regions was placed on a symmetry center ($^1/_2$, 0, 0) (2*d*). We thus concluded that this nitrate was statistically and equally distributed between these two regions. The first "half-nitrate" was described with three atoms N12, O16, and O17 with respective occupancy 0.5, 1, and 0.5. It is disordered between two positions symmetrical with respect to the center and sharing atom O16 and

Table I. Crystal Data and Details of the Structure Determination for $Cu_5(OH)_2(L)_2(NO_3)_4 \cdot 2.5H_2O$

formula	$C_{36}H_{63}N_{12}O_{20.5}Cu_5$
M_r	1309.71
cryst syst	monoclinic
space group	$P2_1/n$
cell params	a = 15.559 (3) Å, b = 13.417 (3) Å, c = 24.638 (8) Å, α = 90°, β = 99.03 (1)°, γ = 90°, V = 5079.1 Å^3, Z = 4
density	1.74 g/cm^3
linear abs	μ = 2.15 mm^{-1}
cryst size	0.15 × 0.15 × 0.30 mm
temp	20 °C
radiation	takeoff angle: 6° wavelength: 0.7107 Å (Mo Kα) monochromator: graphite
bragg angle	$2° < \theta < 25°$
scan	mode: ω range: 0.8 + 0.35 tan θ (deg) speed: from 0.6 to 4 deg/min
detector window	height: 4 mm width: 2.3 + 4.5 tan θ
test reflcns	(740), (722), (808)
measd reflcns	$-15 < h < 15$, $0 < k < 12$, $0 < l < 23$ tot. no.: 9582 F unique > $3\sigma(F)$
refinement	$R = \sum\|\|F_o\| - \|F_c\|\|/\sum\|F_o\|$ $R_w = (\sum w(\|F_o\| - \|F_c\|)^2/\sum w\|F_o\|^2)^{1/2}$ $w = 1/(\sigma^2 + 0.00015\|F\|^2)$ R = 0.049 R_w = 0.062 goodness of fit = 1.72

(7) (a) Brown, D. G.; Reinprecht, J. T.; Vogel, G. C. *Inorg. Nucl. Chem. Lett.* **1976**, *12*, 399–404. (b) Brown, D. G.; Beckman, L.; Hill Ashby, C.; Vogel, G. C.; Reinprecht, J. T. *Tetrahedron Lett.* **1977**, 1363–1364. (c) Brown, D. G.; Vogel, G. C. *Inorg. Chem.* **1978**, *17*, 1367–1368. (d) Brown, D. G.; Hughes, W. J. *Z. Naturforsch., B: Anorg. Chem., Org. Chem.* **1979**, *34b*, 1408–1412. (e) Brown, D. G.; Hughes, W. J.; Knerr, G. *Inorg. Chim. Acta* **1980**, *46*, 123–126.

(8) Kwik, W. L.; Ang, K. P. *Aust. J. Chem.* **1978**, *31*, 459–463.

(9) Andra, K.; Fleischer, F. *Z. Anorg. Allg. Chem.* **1982**, *485*, 210–216.

(10) (a) Speier, G.; Tyeklar, Z. *J. Mol. Catal.* **1980**, *9*, 233–235. (b) Speier, G.; Tyeklar, Z. *J. Chem. Soc., Dalton Trans.* **1983**, 1995–2000. (c) Balogh-Hergovich, E.; Speier, G. *Inorg. Chim. Acta* **1985**, *108*, 59–62.

(11) (a) Muraev, V. A.; Cherkasov, V. K.; Abakumov, G. A.; Razuvaev, G. A. *Dokl. Akad. Nauk SSSR* **1977**, *236*, 620–623. (b) Razuvaev, G. A.; Cherkasov, V. K.; Abakumov, G. A. *J. Organomet. Chem.* **1978**, *160*, 361–371. (c) Abakumov, G. A.; Lobanov, A. V.; Cherkasov, V. K.; Razuvaev, G. A. *Inorg. Chim. Acta* **1981**, *49*, 135–138.

(12) (a) Thompson, J. S.; Calabrese, J. C. *Inorg. Chem.* **1985**, *24*, 3167–3171. (b) Thompson, J. S.; Calabrese, J. C. *J. Am. Chem. Soc.* **1986**, *108*, 1903–1907.

(13) Karlin, K. D.; Gultneh, Y.; Nicholson, T.; Zubieta, J. *Inorg. Chem.* **1985**, *24*, 3725–3727.

(14) Buchanan, R. M.; Wilson-Blumenberg, C.; Trapp, C.; Larsen, S. K.; Green, D. L.; Pierpont, C. G. *Inorg. Chem.* **1986**, *25*, 3070–3076.

(15) Gojon, E.; Greaves, S. J.; Latour, J. M.; Povey, D. C.; Smith, G. W. *Inorg. Chem.*, in press.

(16) Sheldrick, G. M. "SHELX76 Program for Crystal Structure Determination", University of Cambridge: Cambridge, England, 1976.

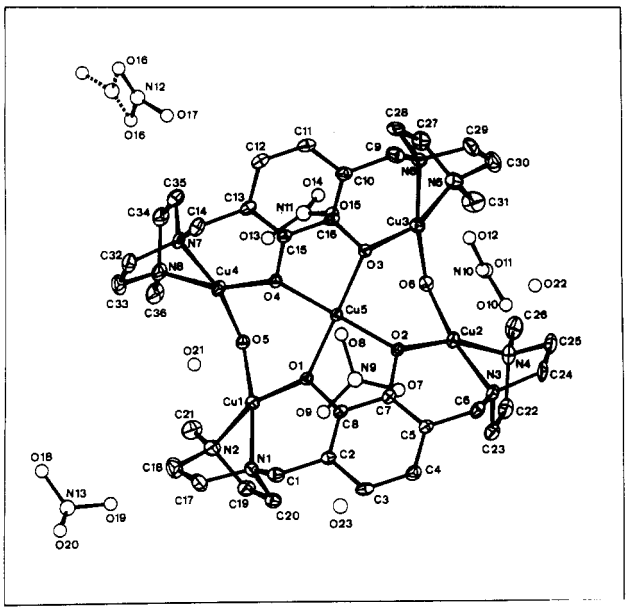

Figure 1. Structure of the pentacopper(II) complex: bottom view showing the numbering scheme.

its symmetrical counterpart. The second "half-nitrate" is in a general position with a half-occupancy. Hydrogen atom positions were calculated with SELX76, except from those of water molecules. Atomic scattering factors and anomalous dispersion terms were taken from the usual sources.[16,17] The final least-squares refinement residue was $R = 0.049$.

The final positional parameters for the non-hydrogen atoms appear in Table II. Tables of general temperature factors (Table III), calculated hydrogen atom positions (Table IV), and structure factor amplitudes (Table V) are available as supplementary material.[18]

Results and Discussion

Synthesis. In the wake of the early work from Robson[19] and Kido[20] introduction of complexing side arms on phenols is generally achieved through formylation and Schiff base formation. However, an alternate procedure was developed recently that is based upon the Mannich condensation of phenols with piperazines.[21] On the other hand, it is known for some time that the Mannich reaction is suitable to introduce aminomethyl groups in the 3- and 6-positions of catechols.[22] By adapting the two literature procedures we have been able to synthesize the new catechol ligand 3,6-bis((4-methylpiperazino)methyl)pyrocatechol, H_2L. This ligand has been characterized by elemental analysis and ^1H and ^{13}C NMR.

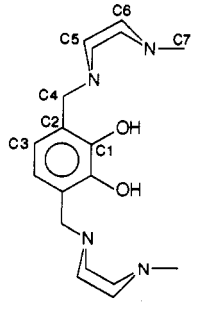

In order to prepare dinuclear complexes we reacted H_2L with 2 equiv of copper nitrate in methanol in the presence of triethylamine. However, from the green reaction mixture the pentanuclear complex $Cu_5(OH)_2(L)_2(NO_3)_4 \cdot 2.5H_2O$ is obtained.

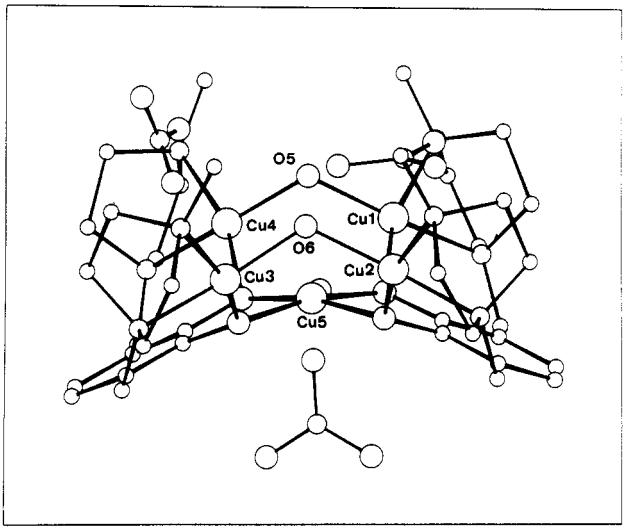

Figure 2. Structure of the pentacopper(II) complex: side view. For the sake of clarity a nitrate and two water molecules have been omitted.

Description of the Structure of $Cu_5(OH)_2(L)_2(NO_3)_4 \cdot 2.5H_2O$. Figure 1 presents an ORTEP view of the complex and the numbering scheme. Figure 2 shows the structure of the cluster. Bond distances and angles are given in Tables VI and VII, respectively. The overall molecule results from the association of two dinuclear units (Cu1Cu2 and Cu3Cu4), which are linked by the two hydroxides and the fifth copper atom (Cu5). From the approximate C_{2v} symmetry of the pentanuclear cluster it follows that the four lateral sites are equivalent while the apical one (Cu5) is unique. Each catechol ligand binds two copper atoms through two piperazine nitrogens and a catecholate oxygen. The fourth equatorial ligand of such copper atoms is a hydroxide ion. These four copper sites are distorted toward tetrahedral geometry from square planar. The dihedral angles between the N_2Cu and O_2Cu planes (for example N1N2Cu1 and O1O5Cu1) are about 16°. The two copper–oxygen bond lengths differ by 0.1 Å with the Cu–O(H) one being shorter (Table VI). The copper–nitrogen bond distances are rather long and, similarly, differ from one another by 0.07 Å; this probably reflects the strain in the piperazine moiety. The same effect was noted by Murray[21b] for the dicopper complex of a piperazine–phenol ligand. The coordination of Cu5 contrasts with the one of the four others since it is roughly square pyramidal with the copper 0.19 Å out of the plane of the four catecholate oxygens. This displacement results from the interaction of the copper with a nitrate oxygen (Cu5–O8 = 2.66 Å). The two other oxygens of this nitrate also interact with Cu1 and Cu2 (Cu1–O9 = 2.69, Cu2–O7 = 2.63 Å). Similarly, two other nitrates are involved in loose bridging of copper pairs: the second nitrate bridges Cu2 and Cu3 through a single oxygen atom O11, while the third one interacts with Cu3 and Cu4 through the three-atom bridge O13–N11–O15. Finally, the oxygen of a water molecule O21 interacts with Cu1 and Cu4. The corresponding Cu–O distances are in the range 2.5–2.9 Å (Table VI). So this nitrate and water bonding completes the coordination of the lateral and apical coppers to 4 + 2 and 4 + 1, respectively.

The five copper atoms in the cluster are arranged as a rectangular based pyramid with Cu5 at the apex of the pyramid (Table VIII). The distances from the apical copper Cu5 to the four others average to 3.46 Å. The lengths of the short Cu–Cu edges (Cu1–Cu4, Cu2–Cu3) of the rectangle that involves the hydroxide bridges are 3.28 Å. On the other hand, the lengths of the long ones (Cu1–Cu2, Cu3–Cu4) inside the dinuclear unit are 5.77 Å. This distance is to be compared with the one observed, 3.25 Å, in the complex described by Karlin where the tetrachlorocatecholate bridges the two copper atoms.[13] In the latter case, the two coppers are located on opposite sides of the catecholate plane, which is twisted from the Cu–Cu axis with an angle of 63°. In the present case, the two coppers are on the same side

(17) *International Tables for X-ray Crystallography*; Kynoch: Birmingham, England, 1974; Vol. IV.
(18) See paragraph at end of paper regarding supplementary material.
(19) Robson, R. *Inorg. Nucl. Chem. Lett.* **1970**, *6*, 125–128.
(20) Okawa, H.; Kida, S. *Bull. Chem. Soc. Jpn.* **1971**, *44*, 1172.
(21) (a) Hodgkin, J. H. *Aust. J. Chem.* **1984**, *37*, 2371–2378. (b) Fallon, G. D.; Murray, K. S.; Spethmann, B.; Yandell, J. K.; Hodgkin, J. H.; Loft, B. C. *J. Chem. Soc., Chem. Commun.* **1984**, 1561–1563.
(22) Fields, D. L.; Miller, J. B.; Reynolds, D. D. *J. Org. Chem.* **1964**, *29*, 2640–2647.

Table II. Atomic Positional Parameters ($\times 10^6$) for $Cu_5(OH)_2(L)_2(NO_3)_4 \cdot 2.5H_2O$

	x	y	z	B_{eq}, Å^2		x	y	z	B_{eq}, Å^2
Cu1	−758 (1)	−1298 (1)	1520 (0)	3.62	N12	234 (9)	−4861 (15)	4988 (6)	7.60
Cu2	1196 (1)	2159 (1)	2398 (3)	3.62	N13	−927 (11)	−5629 (14)	332 (7)	10.40
Cu3	968 (1)	1468 (1)	3650 (0)	4.23	C1	626 (6)	−1759 (6)	839 (4)	4.20
Cu3	−1020 (1)	−1925 (1)	2764 (0)	3.71	C2	1103 (5)	−844 (6)	1075 (3)	3.06
Cu5	646 (1)	−293 (1)	2622 (0)	2.77	C3	1709 (5)	−414 (7)	782 (3)	3.62
O1	412 (3)	−853 (4)	1892 (2)	3.00	C4	2180 (5)	408 (7)	1002 (3)	4.15
O2	1325 (3)	701 (4)	2298 (2)	3.00	C5	2067 (5)	825 (6)	1509 (3)	3.44
O3	1069 (3)	102 (4)	3369 (2)	3.26	C6	2590 (5)	1700 (7)	1746 (4)	3.81
O4	187 (3)	−1437 (4)	2951 (2)	2.99	C7	1459 (5)	379 (6)	1792 (3)	2.79
O5	−1317 (3)	−1102 (4)	2143 (2)	3.37	C8	977 (5)	−457 (6)	1580 (3)	2.93
O6	502 (3)	2032 (4)	2966 (2)	3.57	C9	1940 (6)	185 (8)	4520 (4)	5.41
O7	−267 (4)	1918 (5)	1722 (3)	5.65	C10	1424 (5)	−697 (7)	4260 (3)	3.85
O8	−722 (3)	864 (4)	2290 (3)	5.05	C11	1353 (6)	−1562 (8)	4570 (4)	4.49
O9	−1059 (4)	666 (5)	1396 (3)	5.84	C12	936 (6)	−2382 (8)	4346 (4)	4.23
O10	3553 (4)	1694 (6)	2989 (3)	6.84	C13	535 (5)	−2374 (7)	3793 (3)	3.41
O11	2338 (4)	2055 (5)	3278 (3)	5.60	C14	79 (5)	−3286 (6)	3536 (4)	3.86
O12	3256 (5)	1040 (6)	3707 (4)	8.53	C15	566 (4)	−1514 (6)	3485 (3)	2.91
O13	−1716 (8)	−183 (9)	3270 (5)	14.67	C16	1030 (5)	−685 (6)	3715 (3)	3.46
O14	−1722 (11)	1068 (15)	3747 (7)	25.63	C17	−781 (7)	−2587 (8)	621 (4)	5.86
O15	−698 (9)	624 (16)	3634 (6)	24.09	C18	−1726 (7)	−2474 (9)	708 (5)	6.46
O16	−413 (7)	−4519 (8)	4684 (4)	13.63	C19	−1674 (6)	−750 (8)	489 (4)	4.45
O17	948 (7)	−4673 (14)	4851 (7)	11.27	C20	−690 (6)	−835 (7)	441 (3)	4.23
O18	−1257 (13)	−6004 (16)	710 (9)	12.79	C21	−2728 (6)	−1280 (10)	1042 (4)	6.97
O19	−702 (20)	−4748 (14)	396 (11)	21.64	C22	882 (6)	3692 (8)	1622 (4)	5.58
O20	−431 (22)	−6174 (18)	120 (12)	19.67	C23	1459 (6)	2914 (7)	1409 (4)	4.80
O21	−420 (4)	−2969 (4)	1966 (2)	4.98	C24	2553 (6)	3343 (7)	2172 (4)	4.86
O22	6330 (5)	333 (6)	3449 (3)	9.22	C25	1946 (6)	4017 (7)	2436 (4)	5.45
O23	8956 (12)	1944 (14)	472 (7)	23.24	C26	415 (7)	4287 (8)	2478 (5)	6.81
N1	−322 (5)	−1642 (5)	821 (3)	4.14	C27	216 (7)	2158 (8)	4543 (4)	6.38
N2	−1852 (5)	−1438 (7)	924 (3)	4.70	C28	665 (7)	1202 (8)	4697 (4)	6.54
N3	2030 (4)	2512 (5)	1890 (3)	3.67	C29	2016 (7)	2018 (9)	4618 (4)	6.75
N4	1034 (5)	3661 (5)	2237 (3)	4.64	C30	1541 (8)	2934 (9)	4416 (5)	7.30
N5	657 (5)	2627 (6)	4122 (3)	5.96	C31	153 (8)	3489 (8)	3864 (5)	8.06
N6	1466 (5)	1144 (6)	4422 (3)	4.79	C32	−1304 (6)	−3903 (7)	3017 (4)	5.45
N7	−848 (4)	−3036 (5)	3309 (3)	3.90	C33	−2154 (6)	−3522 (8)	2696 (4)	5.97
N8	−2242 (4)	−2458 (6)	2842 (3)	4.86	C34	−2253 (6)	−2399 (8)	3446 (4)	5.17
N9	−680 (5)	1151 (6)	1791 (4)	4.99	C35	−1352 (5)	−2715 (7)	3739 (4)	4.83
N10	3040 (6)	1590 (6)	3323 (4)	5.10	C36	−3019 (6)	−1986 (8)	2538 (5)	6.09
N11	−1367 (9)	411 (12)	3579 (5)	12.01					

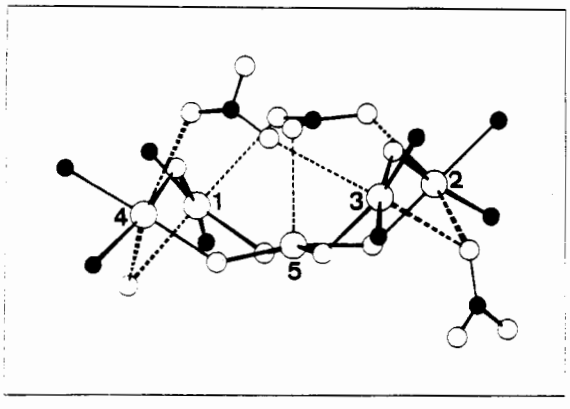

Figure 3. Structure of the pentacopper(II) complex showing only the nitrogen and oxygen atoms surrounding the copper ions. The nitrogen atoms are represented as full circles, the oxygen atoms are represented as open circles, and the copper atoms are numbered.

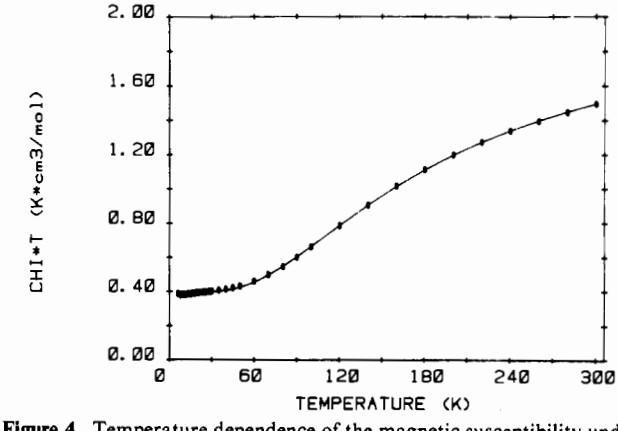

Figure 4. Temperature dependence of the magnetic susceptibility under the form of the χT vs. T curve: (●) experimental points; (–) theoretical curve.

of the catecholate, which is parallel to the Cu–Cu axis. These observations reveal that a catecholate bridge can adopt fairly different geometries to accommodate widely different Cu–Cu distances.

Examination of Table VI shows that mean C–O bond lengths are 1.36 Å and (O)C–C(O) distances are 1.39 and 1.40 Å, which is consistent with values found in other catecholate complexes and confirms the copper(II) catecholate (vs. copper(I) semiquinone) formulation.[5,14]

Finally, it is worth noting that the shortest intermolecular copper–copper distance is 5.99 Å between the apical copper of one molecule, Cu5, and one edge, Cu2, of another. The shortest distance between two apical coppers is 8.93 Å.

Magnetic Susceptibility Study. The temperature dependence of the magnetic susceptibility of the complex is depicted in Figure 4 in the form of the product χT vs. T over the range 5–300 K. Two domains are clearly distinguished. At temperatures lower than 50 K the product χT exhibits a plateau at 0.38 K cm^3/mol. This indicates the presence of an effective spin $^1/_2$ per pentacopper cluster molecule in this temperature range. In the upper temperature domain the product χT increases, which suggests the presence of some antiferromagnetic interaction.

The data has been interpreted in two steps: first, a very simple model was built upon a few hypotheses, and second, the validity of the results has been checked by using a more complete treatment. Furthermore, an EPR study has been performed to discriminate between the possible interpretations.

Consideration of the cluster symmetry along with a few ad-

Table VI. Bond Lengths (Å) for $Cu_5(OH)_2(L)_2(NO_3)_4 \cdot 2.5H_2O$

Cu1–O1	1.998 (4)	C26–N4	1.471 (14)
Cu1–O5	1.898 (5)	C31–N5	1.483 (13)
Cu1–N1	2.001 (7)	C36–N8	1.463 (11)
Cu1–N2	2.075 (7)	C2–C3	1.399 (11)
Cu1–O9	2.687 (6)	C3–C4	1.388 (12)
Cu1–O21	2.516 (5)	C4–C5	1.405 (11)
Cu2–O2	1.986 (5)	C5–C7	1.395 (11)
Cu2–O6	1.905 (5)	C7–C8	1.405 (10)
Cu2–N3	1.996 (7)	C8–C2	1.390 (10)
Cu2–N4	2.062 (6)	C1–C2	1.503 (11)
Cu2–O7	2.622 (6)	C5–C6	1.494 (11)
Cu2–O11	2.582 (6)	C9–C10	1.516 (13)
Cu3–O3	1.974 (5)	C13–C14	1.503 (11)
Cu3–O6	1.885 (4)	C10–C11	1.403 (13)
Cu3–N6	1.986 (7)	C11–C12	1.350 (14)
Cu3–N5	2.045 (8)	C12–C13	1.407 (11)
Cu3–O11	2.572 (7)	C13–C15	1.386 (11)
Cu3–O15	2.825 (15)	C15–C16	1.397 (10)
Cu4–O4	1.975 (4)	C16–C10	1.386 (9)
Cu4–O5	1.885 (4)	C1–N1	1.479 (12)
Cu4–N7	1.996 (7)	C6–N3	1.473 (11)
Cu4–N8	2.068 (6)	C9–N6	1.484 (13)
Cu4–O13	2.935 (12)	C14–N7	1.502 (9)
Cu4–O21	2.697 (5)	C17–N1	1.500 (12)
Cu5–O1	1.930 (4)	C18–N2	1.512 (15)
Cu5–O2	1.949 (5)	C19–N2	1.473 (13)
Cu5–O3	1.929 (4)	C20–N1	1.486 (10)
Cu5–O4	1.925 (5)	C22–N4	1.497 (12)
Cu5–O8	2.660 (5)	C23–N3	1.468 (11)
N9–O7	1.239 (10)	C24–N3	1.487 (11)
N9–O8	1.300 (12)	C25–N4	1.504 (11)
N9–O9	1.240 (10)	C27–N5	1.472 (13)
N10–O10	1.241 (12)	C28–N6	1.511 (14)
N10–O11	1.248 (10)	C29–N6	1.487 (13)
N10–O12	1.205 (12)	C30–N5	1.508 (13)
N11–O13	1.175 (18)	C32–N7	1.488 (11)
N11–O14	1.151 (24)	C33–N8	1.484 (13)
N11–O15	1.067 (20)	C34–N8	1.493 (12)
N12–O16	1.161 (20)	C35–N7	1.478 (12)
N12–O17	1.237 (19)	C17–C18	1.526 (15)
N13–O18	1.239 (29)	C19–C20	1.558 (13)
N13–O19	1.236 (27)	C22–C23	1.523 (14)
N13–O20	1.237 (36)	C24–C25	1.525 (14)
C8–O1	1.363 (9)	C27–C28	1.481 (15)
C7–O2	1.366 (9)	C29–C30	1.480 (16)
C16–O3	1.365 (9)	C32–C33	1.519 (12)
C15–O4	1.359 (8)	C34–C35	1.532 (11)
C21–N2	1.453 (12)		

ditional hypotheses allows us to propose a simple model that fully accounts for the magnetic susceptibility data. First, it is assumed that the apical copper (Cu5) does not interact significantly with the four others. This hypothesis is probably the most questionable; it will be discussed in more detail below. Second, the two hydroxide bridged pairs of coppers are not identical since there is a difference of 1.9° in the CuO(H)Cu bridge angles (Cu1–O5–Cu4 = 119.80, Cu2–O6–Cu3 = 121.68°). According to the magnetostructural correlations established by Hatfield and Hodgson for dihydroxy bridged dicopper complexes such a difference produces changes of about 65 cm^{-1} in the exchange integral.[23] Third, all other interactions are supposedly negligible. Actually, interaction through the catechol ligand between Cu1 and Cu2 and between Cu3 and Cu4 is likely to be negligible since it must involve a five-bond nonplanar pathway. On the basis of these hypotheses, the pentacopper(II) cluster was taken as the sum of a monomer and two different dimers and its magnetic susceptibility was compared to the theoretical expression

$$\chi_{calcd} = \frac{N\beta^2 g_1^2}{4k(T-\Theta)} + \frac{2N\beta^2 g_2^2}{3kT}\left[1 + \frac{1}{3}e^{-2J_1/kT}\right] + \frac{2N\beta^2 g_3^2}{3kT}\left[1 + \frac{1}{3}e^{-2J_2/kT}\right] + 2N\alpha \quad (1)$$

The results of the least-square fitting process are $g_1 = 2.04$, $\Theta = 0.064$ K, $g_2 = 2.04$, $J_1 = -147$ cm^{-1}, $g_3 = 2.06$, $J_2 = -87$ cm^{-1}, and $2N\alpha = 2.5 \times 10^{-4}$ cm^3/mol. The theoretical curve is the solid line in Figure 4. Two points are worth mentioning at this stage. First, when the two dinuclear exchange integrals are forced to be equal in the calculation, the resulting fit is worsened by more than an order of magnitude. This is in line with our second hypothesis that the difference in the CuO(H)Cu angles must produce a difference in the corresponding exchange integrals. Second, the low value of the Weiss constant, $\Theta = 0.064$ K, is in agreement with the first hypothesis that Cu5 does not interact significantly with the four other coppers.

This last observation is in apparent contradistintion with literature data on hydroxide-[23] and alkoxide-bridged[24] dicopper complexes, which predict a strong interaction in such a case. So, to further check this particular point we performed calculations using a recently developed method.[25] In these calculations the second and third hypotheses were conserved but a possible interaction of Cu5 with the other coppers was explicitly taken into account. The structural data indicate that, if operative, these four interactions are identical. This led to the following Hamiltonian:

$$\mathcal{H}_0 = -2J_{14}\vec{S}_1\cdot\vec{S}_4 - 2J_{23}\vec{S}_2\cdot\vec{S}_3 - 2J_{15}(\vec{S}_1\cdot\vec{S}_5 + \vec{S}_2\cdot\vec{S}_5 + \vec{S}_3\cdot\vec{S}_5 + \vec{S}_4\cdot\vec{S}_5) \quad (2)$$

The calculation performed by using the variables g, $2N\alpha$, J_{14}, J_{23}, and $J_{15} = J_{35} = J_{45}$ does not provide a single set of values. Actually, from the statistical test of the minimization process, several groups of values can equally reproduce the experimental data. These are contained in a domain whose limits are as follows:

$g = 2.006$	$g = 2.006$
$2N\alpha = 6.26 \times 10^{-4}$ cm^3 mol^{-1}	$2N\alpha = 6.42 \times 10^{-4}$ cm^3 mol^{-1}
$J_{14} = -161$ cm^{-1}	$J_{14} = -130$ cm^{-1}
$J_{23} = -87$ cm^{-1}	$J_{23} = -75$ cm^{-1}
$J_{15} = -0.8$ cm^{-1}	$J_{15} = -26$ cm^{-1}

This kind of uncertainty in the values deduced from fitting magnetic susceptibility data has already been noted for a tricopper system.[26] It is apparent that the results obtained with the simple model are close to the first set of values deduced from the more complete treatment. However, the latter leads to some ambiguity as to whether the apical copper is actually interacting with the others. Taken alone, the magnetic susceptibility data cannot answer this question. We have thus undertaken an EPR study to investigate this problem.

EPR Spectroscopy. The EPR spectra of the cluster as a polycrystalline powder and as a frozen methanol solution are depicted in Figure 5. Both spectra are not identical, which may result from slight modifications between the solid and the solution species. Nevertheless, the same dominant features are present in both spectra. The lines are very broad, with the low-field region better resolved. The latter feature is most easily observed in the frozen solution spectrum where dilution can, at least partly, lessen intercluster interactions. Two lines are distinguishable in the low-field region, which may be taken as belonging to the quartet due to the hyperfine coupling with a copper atom. A $A_\parallel$ value of 16 mT can be estimated for the coupling, and apparent $g_\parallel$ of 2.21 for the solid and 2.17 for the frozen solution are obtained. At high field the line is extremely broad, but an average apparent $g_\perp$ value of 1.98 can be considered.[27] These parameters are consistent with those observed for a single copper atom in a tetragonal environment.[28] In the simple model presented above

(23) Crawford, V. H.; Richardson, H. W.; Wasson, J. R.; Hodgson, D. J.; Hatfield, W. E. *Inorg. Chem.* **1976**, *15*, 2107–2110.
(24) Nieminen, K. *Ann. Acad. Sci. Fenn., Ser. A2* **1983**, *197*, 1–60.
(25) (a) Belorizky, E.; Fries, P. H. *Nouv. J. Chim.*, in press. (b) Belorizky, E.; Fries, P. H.; Gojon, E.; Latour, J. M. *Mol. Phys.*, in press.
(26) Benelli, C.; Bunting, R. K.; Gatteschi, D.; Zanchini, C. *Inorg. Chem.* **1984**, *23*, 3074–3076.
(27) Due to the broadness of this line, it is not possible to exclude that the g tensor is rhombic. Nevertheless, this hypothesis is not supported by the structural data, which shows little departure of the copper sites from tetragonality.
(28) Hathaway, B. J.; Billig, D. E. *Coord. Chem. Rev.* **1970**, *5*, 143–207.

Table VII. Bond Angles (deg) for $Cu_5(OH)_2(L)_2(NO_3)_4 \cdot 2.5H_2O$

O1–Cu1–O5	95.1 (2)	N6–Cu3–O3	95.3 (2)	O8–Cu5–O2	86.2 (1)	C22–N4–C25	108.2 (7)
O5–Cu1–N2	99.0 (2)	O3–Cu3–N5	160.8 (2)	O8–Cu5–O3	105.6 (2)	C27–N5–C30	105.6 (7)
N2–Cu1–N1	73.8 (3)	O6–Cu3–N6	168.9 (2)	O8–Cu5–O4	105.3 (1)	C33–N8–C34	108.0 (7)
N1–Cu1–O1	93.2 (2)	O11–Cu3–O6	77.4 (2)	C2–C3–C4	119.0 (7)	C18–C17–N1	106.8 (8)
O1–Cu1–N2	160.0 (2)	O11–Cu3–N5	104.7 (2)	C3–C4–C5	122.2 (7)	C19–C20–N1	107.0 (7)
O5–Cu1–N1	171.2 (2)	O11–Cu3–N6	100.8 (2)	C4–C5–C7	117.6 (7)	C22–C23–N3	106.8 (7)
O9–Cu1–O1	83.6 (2)	O11–Cu3–O3	92.5 (2)	C5–C7–C8	121.4 (7)	C25–C24–N3	108.3 (7)
O9–Cu1–O5	82.1 (2)	O15–Cu3–O6	85.7 (3)	C7–C8–C2	119.3 (7)	C27–C28–N6	108.6 (8)
O9–Cu1–N2	84.2 (2)	O15–Cu3–N5	90.8 (4)	C8–C2–C3	120.6 (7)	C30–C29–N6	108.3 (8)
O9–Cu1–N1	101.8 (2)	O15–Cu3–N6	98.3 (3)	C10–C11–C12	121.7 (8)	C33–C32–N7	107.4 (7)
O21–Cu1–O1	87.3 (2)	O15–Cu3–O3	75.3 (4)	C11–C12–C13	120.1 (9)	C34–C35–N7	107.0 (7)
O21–Cu1–O5	82.0 (2)	O11–Cu3–O15	158.2 (3)	C12–C13–C15	119.2 (8)	C17–C18–N2	108.8 (8)
O21–Cu1–N2	108.7 (2)	O4–Cu4–O5	95.6 (2)	C13–C15–C16	120.1 (6)	C20–C19–N2	108.0 (7)
O21–Cu1–N1	95.4 (2)	O5–Cu4–N8	99.6 (2)	C15–C16–C10	120.4 (7)	C23–C22–N4	108.8 (7)
O9–Cu1–O1	83.6 (2)	N8–Cu4–N7	73.0 (2)	C16–C10–C11	118.4 (7)	C24–C25–N4	106.8 (7)
O2–Cu2–O6	94.8 (2)	N7–Cu4–O4	93.9 (2)	C2–C8–O1	123.6 (6)	C28–C27–N5	107.3 (8)
O6–Cu2–N4	99.4 (2)	O4–Cu4–N8	161.4 (2)	C5–C7–O2	122.2 (6)	C29–C30–N5	107.7 (9)
N4–Cu2–N3	73.7 (3)	O5–Cu4–N7	166.8 (2)	C10–C16–O3	123.9 (7)	C32–C33–N8	107.7 (7)
N3–Cu2–O2	93.9 (2)	O13–Cu4–O5	79.5 (2)	C13–C15–O4	123.1 (6)	C35–C34–N8	107.6 (7)
O2–Cu2–N4	161.9 (2)	O13–Cu4–N8	80.2 (3)	C7–C8–O1	117.1 (6)	O7–N9–O8	118.7 (7)
O6–Cu2–N3	168.9 (2)	O13–Cu4–N7	109.2 (3)	C8–C7–O2	116.3 (6)	O8–N9–O9	119.9 (7)
O7–Cu2–O2	83.9 (1)	O13–Cu4–O4	92.2 (2)	C15–C16–O3	115.7 (6)	O9–N9–O7	121.4 (9)
O7–Cu2–O6	85.4 (2)	O21–Cu4–O5	77.4 (1)	C16–C15–O4	116.8 (6)	O10–N10–O11	122.0 (8)
O7–Cu2–N4	86.0 (2)	O21–Cu4–N8	108.5 (2)	C2–C1–N1	110.8 (6)	O11–N10–O12	120.6 (9)
O7–Cu2–N3	102.5 (2)	O21–Cu4–N7	94.4 (2)	C5–C6–N3	111.6 (6)	O12–N10–O10	117.4 (8)
O11–Cu2–O2	88.9 (2)	O21–Cu4–O4	85.2 (2)	C10–C9–N6	113.1 (7)	O13–N11–O14	123.6 (15)
O11–Cu2–O6	76.9 (2)	O13–Cu4–O21	156.4 (2)	C13–C14–N7	109.7 (6)	O14–N11–O15	105.2 (18)
O11–Cu2–N4	105.2 (2)	O1–Cu5–O2	85.4 (2)	C17–N1–C20	107.0 (6)	O15–N11–O13	127.3 (17)
O11–Cu2–N3	96.3 (2)	O2–Cu5–O3	94.4 (2)	C23–N3–C24	108.6 (6)	O16–N12–O17	116.0 (15)
O7–Cu2–O11	160.3 (2)	O3–Cu5–O4	84.9 (2)	C28–N6–C29	106.7 (7)	O18–N13–O19	115.8 (22)
O3–Cu3–O6	95.7 (2)	O4–Cu5–O1	93.1 (2)	C32–N7–C35	107.9 (6)	O19–N13–O20	115.9 (24)
O6–Cu3–N5	96.4 (2)	O8–Cu5–O1	85.2 (2)	C18–N2–C19	105.7 (7)	O20–N13–O19	115.9 (24)
N5–Cu3–N6	73.3 (3)						

Table VIII. Structural Parameters of the Cu_5 Pyramid

	Bond Distances (Å)		
Cu1–Cu2	5.78	Cu1–Cu5	3.48
Cu3–Cu4	5.74	Cu2–Cu5	3.46
Cu1–Cu4	3.27	Cu3–Cu5	3.44
Cu2–Cu3	3.29	Cu4–Cu5	3.46
	Bond Angles (deg)		
Cu1–Cu2–Cu3	89.87	Cu3–Cu5–Cu4	112.69
Cu2–Cu3–Cu4	89.85	Cu1–Cu5–Cu4	56.17
Cu3–Cu4–Cu1	90.74	Cu2–Cu5–Cu3	56.92
Cu4–Cu1–Cu2	89.52	Cu1–Cu5–Cu3	147.27
Cu1–Cu5–Cu2	112.61	Cu2–Cu5–Cu4	145.69

this signal would correspond to the apical copper Cu5.[29] However, the spectra exhibit additional features in the perpendicular region, indicating the existence of some weak intracluster interactions. These interactions have a maximum of a few tenths of a millitesla and are then much weaker than the Zeeman interaction. In particular, the trough appearing at $g = 1.87$ is unexpected for a single Cu(II) ion. Such a feature has been recently reported to arise from weak dipolar interactions within a pair of uncoupled copper atoms.[30] This interpretation does not apply here, for one cannot expect any dipolar interaction to arise from a pair of antiferromagnetically coupled copper ions near liquid-helium temperatures where only the ground state ($S = 0$) of the pair is populated. Finally, it is worth mentioning that the EPR signal dramatically broadens above 25 K due to the increase in the spin–lattice relaxation rate. In the case of multinuclear iron centers, such a behavior was interpreted as resulting from the population of low-lying excited electronic levels.[31] For this explanation to apply here it is necessary that the apical copper be interacting with the lateral ones.

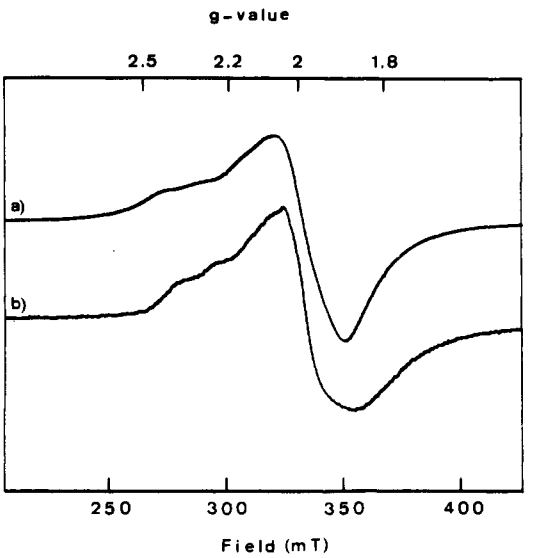

Figure 5. X-Band EPR spectra of $Cu_5(OH)_2(L)_2(NO_3)_4 \cdot 2.5H_2O$ recorded at ca. 20 K: (a) of a polycrystalline sample; (b) of a frozen methanol solution. Spectrometer settings: frequency, 9.241 GHz; modulation frequency, 100 KHz; modulation amplitude, 0.8 mT; power, (a) 10 mW and (b) 200 μW.

In conclusion, this EPR study strongly suggests that some interaction is operative between the apical copper and its four neighbors. However, it is not possible to estimate the extent of the interaction from the present polycrystalline and solution data. This evaluation is only attainable through a complete single-crystal study, which we have not been able to perform with the crystals at hand. As stated above, the interaction is very small, and thus, the simple model that we developed at first can be viewed as a not too unreasonable approximation.

Conclusions of the Magnetic Studies. One can now try to analyze the implications of these results on the molecular level. The first point to be discussed is the difference in the values of

(29) Alternatively, it would correspond to the ground state ($S = {}^1/_2$) of the pentanuclear cluster if Cu5 interacts with its four neighbors.[30]

(30) Gatteschi, D.; Bencini, A. In *Magneto-Structural Correlations in Exchange Coupled Systems*; Willett, R. D., Gatteschi, D., Kahn, O., Eds.; NATO ASI Series; D. Reidel: Dordrecht, The Netherlands; pp 241–267.
(31) Spira-Solomon, D. J.; Allendorf, M. D.; Solomon, E. I. *J. Am. Chem. Soc.* **1986**, *108*, 5318–5328.
(32) Bertrand, P.; Gayda, J. P.; Rao, K. K. *J. Chem. Phys.* **1982**, *76*, 4715–4719.

the two exchange integrals of similar origine, J_{14} and J_{23}. A difference of about 65 cm^{-1} is observed, which is in good agreement with what might be expected from the literature.[23] Due to the symmetry of the cluster, the values of the two exchange integrals deduced from the calculation cannot be unambiguously attributed to a specific pair of copper atoms. The higher value is probably associated with the pair that has the most acute bridge angle Cu1-Cu4 (Cu1-O5-Cu4 = 119.80° vs. Cu2-O6-Cu3 = 121.68°).[23,24] No definite correlation of the magnetic and structural properties has been found for monohydroxy-bridged dicopper complexes. For tetragonal complexes exchange interactions span the range -32 to -500 cm^{-1} while the corresponding CuO(H)Cu angles vary from 110 to 147°.[33] In the present study, intermediate values are obtained for both parameters. It is interesting to note that all but one[33c] data conform to the general trend that the more obtuse the CuO(H)Cu angle, the stronger the antiferromagnetic coupling.[23,24]

The weak interaction of Cu5 with its four neighbors is probably the most surprising result. Consideration of the orientation of the magnetic orbitals ($d_{x^2-y^2}$ for all coppers) would predict that some overalap is possible on the catechols oxygens. Moreover, the magnitude of the Cu5-O-Cu angles seems to warrant that a significant interaction may be operative. We think that the nonplanarity of the system is responsible for the reduced coupling of Cu5. This is better illustrated in Figure 3, which presents only the five copper atoms with their immediate O and N environment. It clearly appears that the coordination plane of Cu5 is not coplanar with the one of any other copper atom. Actually, the dihedral angles between these planes average to 129°. This situation is analogous to the one observed very recently in a tetranuclear copper catecholate.[15] In the latter case, no coupling was present inside a pair of copper atoms despite the fact that a significant overlap of the magnetic orbitals was expected on a bridging oxygen. The absence of coupling was attributed to the fact that the axis of the magnetic orbital (d_{z^2}) of one copper made an angle of 124° with the basal plane of the other. This situation is reminiscent of the folding observed in some dihydroxy-bridged dicopper complexes,[34a] which has been shown theoretically to produce smaller singlet-triplet splittings as a result of decreasing both the ferromagnetic and the antiferromagnetic contributions.[34b]

Conclusions

This publication reports the structural and magnetic characterization of a novel pentacopper(II) cluster built around two molecules of a trinucleating catecholate ligand. To our knowledge this is the second example of a catecholate bonding three metal atoms. We recently found the first one in a compound that resulted from the dimerization of a dicopper complex of a binucleating catecholate.[15] The trinucleating character of the present ligand is obviously the driving force of the molecular assembly and it can probably be used with other metals to obtain clusters of higher nuclearity. Work is currently in progress along these lines.

Acknowledgment. We thank Professor E. Belorizky and Dr. P. Fries for their help in the treatment of the magnetic susceptibility data.

Supplementary Material Available: Listings of general temperature factors (Table III) and calculated hydrogen atom positions (Table IV) (3 pages); a listing of structure factor amplitudes (Table V) (24 pages). Ordering information is given on any current masthead page.

(33) (a) Haddad, M. S.; Wilson, S. R.; Hodgson, D. J.; Hendrickson, D. N. *J. Am. Chem. Soc.* **1981**, *103*, 384-391. (b) Burk, P. L.; Osborn, J. A.; Youinou, M. T. *J. Am. Chem. Soc.* **1981**, *103*, 1273-1274. (c) Coughlin, P. K.; Lippard, S. J. *J. Am. Chem. Soc.* **1981**, *103*, 3228-3229. (d) Drew, G. B.; Mc Cann, M.; Nelson, S. M. *J. Chem. Soc., Dalton Trans.* **1981**, 1868-1878. (e) Drew, G. B.; Nelson, J.; Esho, F.; Mc Kee, V.; Nelson, S. M. *J. Chem. Soc., Dalton Trans.* **1982**, 1837-1843.

(34) (a) Charlot, M. F.; Kahn, O.; Jeannin, S.; Jeannin, Y. *Inorg. Chem.* **1980**, *19*, 1411-1413. (b) Kahn, O.; Charlot, M. F. *Nouv. J. Chim.* **1980**, *4*, 567-576.

Contribution from Chemistry Department A, The Technical University of Denmark, 2800 Lyngby, Denmark

Electron Transfer from Cytochrome *c* to Tris(1,10-phenanthroline)cobalt(III) and Its Electrically Neutral Sulfonated Analogue as a Probe for Direct, Image, and Nonlocal Electrostatic Interactions at the Protein Surface

A. M. Kjaer and J. Ulstrup*

Received August 21, 1986

We have investigated the kinetics of electron transfer between cytochrome c^{II} and the triply charged and electrically neutral $[Co(phen)_3]^{3+}$ and $[Co(phen\text{-}SO_3^-)_3]$ complexes in aqueous Tris, sodium *p*-toluenesulfonate (NaTS), and chloride media at pH 7.00 (phen = 1,10-phenanthroline). The rate constant, activation enthalpy ΔH_A, and apparent activation entropy ΔS_A^{app} of the former in 0.05 mol dm^{-3} Tris/NaTS are 2.92×10^3 dm^3 mol^{-1} s^{-1}, 49 ± 2 kJ, and -15 ± 5 J K^{-1}, respectively, and of the latter are 2.35×10^5 dm^3 mol^{-1} s^{-1}, 30 ± 2 kJ, and -40 ± 5 J K^{-1}, respectively. The rate constants are smaller in media containing protein-binding ions (chloride or phosphate), while ΔH_A is little affected. The reaction of $[Co(phen\text{-}SO_3^-)_3]$ is independent of the ionic strength μ, and thus this species behaves as a neutral molecule, while the reaction of $[Co(phen)_3]^{3+}$ follows a Debye-Hückel law in the μ range 0.1-0.2 mol dm^{-3}. The charge product is 3.2 for nonbinding ions and is lower for binding anions. The data have been analyzed by means of a model in which Co(III) is represented as a conducting sphere embedded in a dielectric and cyt *c* is another dielectric of low dielectric constant. The rate parameters can be understood in terms of reorganization in both dielectric regions and of image force and nonlocal electrostatic work terms. Small electronic transmission coefficients, around 10^{-5}, emerge when the activation entropies are calculated on the basis of the model.

Introduction

We have recently reported a search for electron-transfer systems that might both belong to the diabatic limit and be well-represented by the simplest conceivable models for the reactant ions and solvent[1] resting on a conducting-sphere approximation for the ions interacting through coulombic terms that are screened by a ma-

(1) Kjaer, A. M.; Ulstrup, J. *Inorg. Chem.* **1986**, *25*, 644.

0020-1669/87/1326-2052$01.50/0 © 1987 American Chemical Society